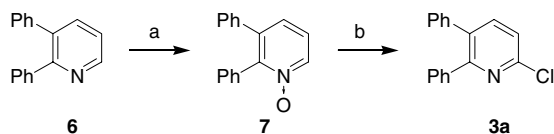


**Scheme 1.** Reagents and conditions for synthesis of **5a–d**: (a) 4-(methylamino)-1-butanol (10 equiv for **3a,b**, and c, 1.5 equiv for **3d**), **3a**, neat, 100 °C; **3b**, neat, 190 °C; **3c**, neat, 170 °C; **3d**, K<sub>2</sub>CO<sub>3</sub>, DMF, rt; (b) BrCH<sub>2</sub>CO<sub>2</sub>*t*-Bu, *n*-Bu<sub>4</sub>NHSO<sub>4</sub>, aq KOH, benzene, 0 °C to rt; (c) 1 N NaOH, MeOH, reflux.

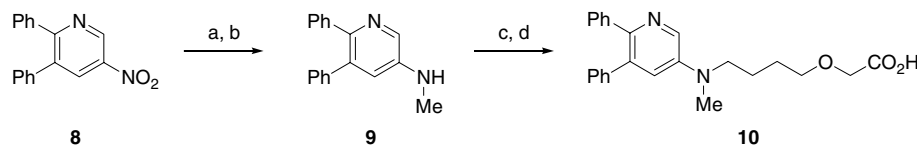
The strategy for the synthesis of diphenylated heterocycles **5a–d**, which is similar to that described for the corresponding pyrazine derivatives,<sup>11</sup> is summarized in Scheme 1. Coupling of **3a–d** with 4-(methylamino)-1-butanol afforded the corresponding alcohols **4a–d**. O-Alkylation of the alcohols **4a–d** with *tert*-butyl bromoacetate under phase-transfer conditions<sup>12</sup> followed by saponification afforded the desired compounds **5a–d**. The starting material **3a** was synthesized by N-oxidation of 2,3-diphenylpyridine **6**<sup>13</sup> and subsequent reaction of the resulting *N*-oxide **7** with phosphorus oxychloride as shown in Scheme 2. Other starting materials **3b**,<sup>14</sup> **c**<sup>15</sup>, and **d**<sup>16</sup> were prepared according to literature procedures.

The synthetic route to the diphenylpyridine **10** is shown in Scheme 3. The requisite pyridine **9** was prepared by catalytic hydrogenation of **8**<sup>17</sup> followed by N-methylation of the resulting amine by reductive alkylation.<sup>18</sup> N-Alkylation of **9** with *tert*-butyl (4-bromobutyl)oxyacetate<sup>11</sup> in the presence of K<sub>2</sub>CO<sub>3</sub> and NaI gave the corresponding ester, which was converted to the target compound **10** by alkaline hydrolysis.

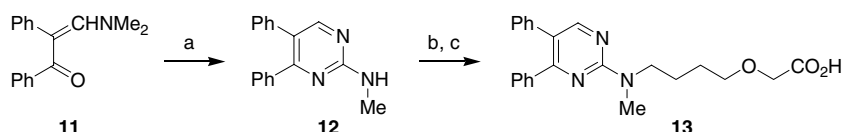
The pyrimidine **13** was synthesized as shown in Scheme 4. Cyclization of 1-methylguanidine and the enamine



**Scheme 2.** Reagents and conditions for synthesis of **3a**: (a) *m*CPBA, CHCl<sub>3</sub>, rt; (b) POCl<sub>3</sub>, 100 °C.



**Scheme 3.** Reagents and conditions for synthesis of **10**: (a) HCO<sub>2</sub>NH<sub>4</sub>, 10% Pd–C, MeOH, rt; (b) i–HCO<sub>2</sub>Et, EtOH, reflux; ii–LiAlH<sub>4</sub>, THF, rt; (c) Br(CH<sub>2</sub>)<sub>4</sub>OCH<sub>2</sub>CO<sub>2</sub>*t*-Bu, K<sub>2</sub>CO<sub>3</sub>, NaI, DMF, 90 °C; (d) 1 N NaOH, MeOH, reflux.



**Scheme 4.** Reagents and conditions for synthesis of **13**: (a) 1-methylguanidine hydrochloride, K<sub>2</sub>CO<sub>3</sub>, xylenes, reflux; (b) i–NaH, DMF, 80 °C; ii–Br(CH<sub>2</sub>)<sub>4</sub>OCH<sub>2</sub>CO<sub>2</sub>*t*-Bu, 0 °C to rt; (c) 1 N NaOH, MeOH, reflux.

**11**<sup>19</sup> gave the 2-(methylamino)pyrimidine **12**, which was N-alkylated with *tert*-butyl (4-bromobutyl)oxyacetate in the presence of sodium hydride as a base, followed by saponification to give the target compound **13**.

The test compounds prepared were evaluated for their potency to inhibit ADP-induced platelet aggregation in human platelet-rich plasma. The concentration of test compound giving 50% inhibition of aggregation (IC<sub>50</sub>) was determined from dose–response curves. In this assay, iloprost, beraprost sodium, and BMY42393 exhibited IC<sub>50</sub> values of 5 nM, 17 nM, and 1.5 μM, respectively. The biological activity of the compounds synthesized is summarized in Table 1.

Using compound **2** as a template, we investigated the effect on biological potency of replacing the diphenylpyrazine ring by various diphenylated 6-membered heteroaromatic rings. Platelet inhibitory activity was considerably affected by modification of the pyrazine ring (Table 1). To gain an understanding of the structural elements required for potency, three pyridine analogues required for potency, three pyridine analogues **5a,b** and **10** were prepared. Replacement of the 2-amino-5,6-diphenylpyrazine ring in **2** with a 2-amino-5,6-diphenylpyridine ring gave **5a**, which retained the potency of **2**. The regioisomeric pyridines **5b** and **10** showed severalfold-reduced potency compared to **2** and **5a**. This result indicates that the nitrogen atom at the 1-position (numbering according to the structure shown in Table 1) has some impact on biological activity. We next synthesized the pyrimidine **13**, the pyridazine **5c**, and the triazine **5d**, which have two or three nitrogen atoms in the 6-membered heteroaromatic ring. The pyrimidine **13** showed a fourfold loss of potency compared with **2**, much the same as **5b** and **10**. A similar

**Table 1.** Effect of alteration of the pyrazine ring of **2** on inhibition of ADP-induced human platelet aggregation

Compound	Het	Inhibition of human platelet aggregation IC <sub>50</sub> (μM) <sup>a</sup>
<b>2</b>		0.2
<b>5a<sup>b</sup></b>		0.2
<b>5b</b>		1.1
<b>5c</b>		8.6
<b>5d</b>		1.3
<b>10<sup>a</sup></b>		0.8
<b>13</b>		0.8

<sup>a</sup> Inhibition of platelet aggregation induced by ADP (10 μM) in human platelet rich-plasma.

<sup>b</sup> The biological activity of the sodium salt was evaluated.

result was obtained for the triazine **5d**. The pyridazine **5c** was substantially less potent than the other analogues, a result that provides evidence for the importance of the nitrogen atom at the 1-position.

To further elucidate their SAR, we performed docking studies for the representative agonists shown in Table 1. Stitham et al.<sup>20</sup> have constructed a 3D model of the IP receptor with the Internet-based protein structure homology-modeling server Swiss Model (<http://swissmodel.expasy.org/>) by using the X-ray crystallographic structure of the bovine rhodopsin receptor (Protein Data Bank code 1HZX) as a template. They have also proposed a docking model for prostacyclin bound to the IP receptor. Our 3D model of the IP receptor was prepared according to their method by using MOE version 2003.01 (Chemical Computing Group, Inc.). The sequences of the IP receptor (Swiss-Prot accession number P43119) and the bovine rhodopsin receptor were aligned as described by Stitham et al.<sup>20</sup> A set of 10 intermediate homology models was generated with the Homology module, and each intermediate was minimized to an energy gradient of 0.01 kcal mol<sup>-1</sup> Å<sup>-1</sup>. The quality of the models generated was validated with the Protein Report module, and the model with the lowest energy was selected for further study.

Stitham et al.<sup>20</sup> showed that mutation of Tyr75, Phe95, Phe278, or Arg279 of the IP receptor to Ala significantly reduces the binding affinity for iloprost, providing evidence that these amino acids are important for binding. Taking this result into account, we manually docked **5a**, which is as active as **2**, into the binding site of the IP receptor by rotating around the single bonds of **5a** and the side chains of the ligand-contacting amino acids in the binding site. We then performed energy minimization with the MMFF94x force field<sup>21</sup> implemented in MOE. Compound **5a** and the amino acids within 7 Å of **5a** were energy-minimized until the root-mean-square gradient of the potential energy was less than 0.1 kcal mol<sup>-1</sup> Å<sup>-1</sup>. An automatic docking study with GLIDE version 3.0 (Schrödinger, Inc.) produced similar binding models. The entire docked model, in which the IP receptor is shown as seven transmembrane (TM) helices, is shown in Figure 2a. Compound **5a** interacts mainly with helices TM1, TM2, TM3, and TM7. Figure 2b shows a close-up view of the binding site of the complex. The carboxyl group of **5a** is located close to the guanidino group of Arg279, so that it is well placed for electrostatic interaction with this amino acid. The nitrogen atom at the 1-position of the pyridine ring is well placed to form a hydrogen bond with the hydroxyl group of Tyr75. The hydroxyl group of Ser20 is likely to form a hydrogen bond with the hydroxyl group of Tyr75, thereby stabilizing the interaction between the 1-position nitrogen atom of **5a** and the hydroxyl group of Tyr75. The amino acids Met23, Leu67, Val71, Phe95, Met99, Phe102, Phe278, Ala282, and Pro285 form a large hydrophobic pocket which accommodates well the two phenyl groups of **5a**, and van der Waals interactions between the hydrophobic side chains of the amino acids and the phenyl groups of **5a** are facilitated. Similar modes of interaction were observed in the docking model for prostacyclin bound to the IP receptor<sup>20</sup>: the carboxyl group of prostacyclin interacts with the guanidino group of Arg279 and the hydroxyl group at C11 interacts with the hydroxyl group of Tyr75, while the hydrophobic methylene chain is located close to the hydrophobic amino acids mentioned above.

The pyridine derivatives **5b** and **10** do not have nitrogen atoms at the 1-position, yet they were fairly active. To investigate the reason for this, we docked **5b** into the binding site of the IP receptor and found that it bound well when it was flipped so that the nitrogen atom at the 3-position could interact with the hydroxyl group of Tyr75 (Fig. 2c). When compound **10** was similarly docked (Fig. 2d), the nitrogen atom at the 4-position could interact with the hydroxyl group of Ser20 instead of that of Tyr75, and the hydroxyl group of Tyr75 apparently forms a hydrogen bond with the hydroxyl group of Ser20. This flipping of **5b** and **10** does not greatly affect the mode of interaction of the substituents at the 2-, 5-, and 6-positions with the IP receptor. In **5a**, the carboxyl group is located close to the guanidino group of Arg279, and the two phenyl groups at the 5- and 6-positions interact with the hydrophobic pocket formed by Met23, Leu67, Val71, Phe95, Met99, Phe102, Phe278, Ala282, and Pro285. The flexible methylene chain of the substituent at the 2-position can easily

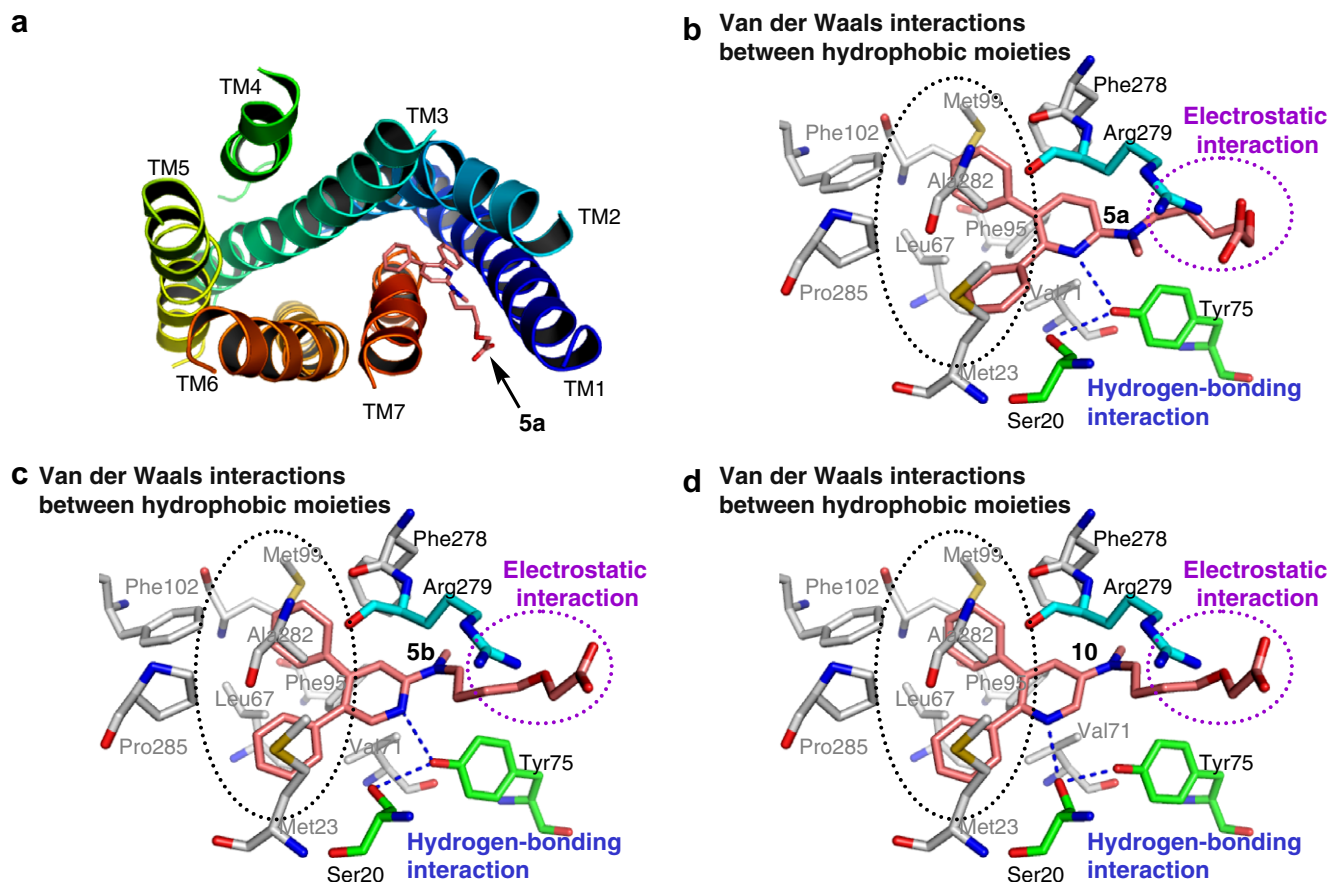


**Figure 2.** Docking models of the homology-modeled IP receptor in complex with **5a**, **5b**, or **10**. Hydrophobic amino acids are shown in white, and hydrogen-bonding interactions are shown as broken lines. The figure was prepared with PyMOL version 0.99 (DeLano Scientific).

adapt its conformation so that the terminal carboxyl group can interact with the guanidino group of Arg279. Because the substituents at the 5- and 6-positions are the same, the flipping of **5b** or **10** does not significantly affect the interactions of these substituents with the IP receptor.

Lead compound **2** can be docked into the IP receptor in the same manner as **5a** or **10** (Fig. 2b and d). Though it is difficult to determine which nitrogen atom of the pyrazine ring interacts with the hydroxyl group of Tyr75 or Ser20, it is reasonable to assume that a **5a**-type interaction (Fig. 2b) is more probable than a **10**-type interaction (Fig. 2d) because **5a** is more potent than **10**.

Similarly, **13** can be docked into the receptor in the same manner as **5a** or **5b** (Fig. 2b and c). In **13**, a **5a**-type interaction is more plausible than a **5b**-type interaction, because **5a** is more potent than **5b**.

The result for **5c** is less clear, because this compound has lower activity than **5b** or **10**. Electrostatic-potential maps are widely used in drug design to evaluate electronic properties.<sup>22</sup> We therefore calculated electrostatic-potential maps of the 6-membered heteroaromatic rings by using a Hartree–Fock quantum mechanical model with a 6-31G(\*) basis set with Trident software (Wavefunction, Inc.). To avoid excessively long

computation times, we replaced the phenyl groups and the carboxylate side chain with simple methyl groups, which are unlikely to greatly influence the electronic environment of the heteroaromatic rings. In the electrostatic-potential maps (Fig. 3), the colors range from red

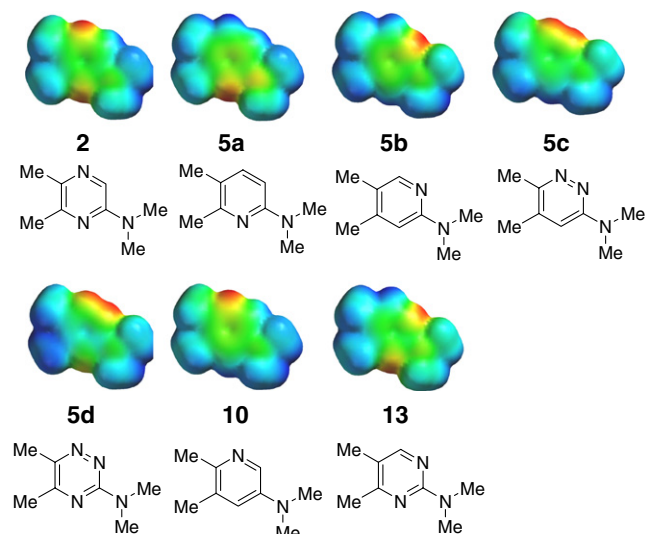


**Figure 3.** Electrostatic-potential maps of the central heteroaromatic rings of test compounds calculated with a 6-31G(\*) basis set.

(high electronegativity) through green to blue (high electropositivity). The electrostatic-potential map of **5c** clearly differs from those of **2**, **5a**, **5b**, **10**, and **13**, in that the adjacent location of the two nitrogen atoms greatly increases the red area around the nitrogen atoms. In the IP receptor, the hydroxyl groups of Ser20 and Tyr75 are close together and form an electronegative environment. The electronegativity of the two adjacent nitrogen atoms in **5c** may lead to unfavorable electronic interactions between the nitrogen atoms and the electronegative hydroxyl groups of Ser20 and Tyr75, thereby weakening the hydrogen-bonding interaction between them. Even though **5d** also has two adjacent nitrogen atoms, it is more active than **5c**. This is reasonable because **5d** also has a nitrogen atom at the 1-position, so that a **5a**-type interaction is possible.

Our results can be summarized as follows. (1) The important interactions with the IP are the same for prostacyclin and the diphenylpyrazine derivatives: electrostatic interactions between the terminal carboxyl group and the guanidino group of Arg279, hydrogen-bonding interactions between a nitrogen atom of the heteroaromatic ring and the hydroxyl group of Ser20 or Tyr75, and van der Waals interactions with the hydrophobic side chains of Met23, Leu67, Val71, Phe95, Met99, Phe102, Phe278, Ala282, and Pro285. (2) The flexibility of the substituent at the 2-position and the presence of the same group at the 5- and 6-positions allow two modes of binding depending on the position of the nitrogen atom in the heteroaromatic ring. (3) A favorable hydrogen-bonding interaction between a nitrogen atom of the heteroaromatic ring and Ser20 or Tyr75 greatly contributes to the agonistic activity.

In conclusion, we have described the synthesis and the SAR associated with novel nonprostanoid IP receptor agonists, with emphasis on the pyrazine ring of lead compound **2**. The results of a molecular-modeling study provide a rationale for the observed SAR, and identify the interactions important for agonistic activity. To our knowledge, the present docking models are the first ones constructed for nonprostanoid IP receptor agonists. This type of study is expected to open new perspectives for the rational design of nonprostanoid-type IP receptor agonists.

#### Acknowledgment

We thank Dr. Gerald E. Smyth for helpful suggestions during the preparation of the manuscript.

#### References and notes

- Moncada, S.; Gryglewski, R.; Bunting, S.; Vane, J. R. *Nature* **1976**, *263*, 663.
- Moncada, S.; Vane, J. R. *Pharmacol. Rev.* **1978**, *30*, 293.
- Barst, R. J.; Rubin, L. J.; Long, W. A.; McGoon, M. D.; Rich, S.; Badesch, D. B.; Groves, B. M.; Tapson, V. F.; Bourge, R. C.; Brundage, B. H.; Koerner, S. K.; Langleben, D.; Keller, C. A.; Murali, S.; Uretsky, B. F.; Clayton, L. M.; Jöbsis, M. M.; Blackburn, S. D., Jr.; Shortino, D.; Crow, J. W. *N. Engl. J. Med.* **1996**, *334*, 296.
- Skuballa, W.; Vorbrüggen, H. *Angew. Chem., Int. Ed. Engl.* **1981**, *20*, 1046.
- Skuballa, W.; Schillinger, E.; Stürzebecher, C.-S.; Vorbrüggen, H. *J. Med. Chem.* **1986**, *29*, 313.
- Ohno, K.; Nagase, H.; Matsumoto, K.; Nishigama, H.; Nishio, S. *Adv. Prostaglandin Thromboxane Leukotriene Res.* **1985**, *15*, 279.
- Meanwell, N. A.; Rosenfeld, M. J.; Trehan, A. K.; Wright, J. J. K.; Brassard, C. L.; Buchanan, J. O.; Federici, M. E.; Fleming, J. S.; Gamberdella, M.; Zavoico, G. B.; Seiler, S. M. *J. Med. Chem.* **1992**, *35*, 3483.
- Meanwell, N. A.; Romine, J. L.; Rosenfeld, M. J.; Martin, S. W.; Trehan, A. K.; Wright, J. J. K.; Malley, M. F.; Gougoutas, J. Z.; Brassard, C. L.; Buchanan, J. O.; Federici, M. E.; Fleming, J. S.; Gamberdella, M.; Hartl, K. S.; Zavoico, G. B.; Seiler, S. M. *J. Med. Chem.* **1993**, *36*, 3884.
- Hamanaka, N.; Takahashi, K.; Nagao, Y.; Torisu, K.; Tokumoto, H.; Kondo, K. *Bioorg. Med. Chem. Lett.* **1995**, *5*, 1083.
- Hattori, K.; Tabuchi, S.; Okitsu, O.; Taniguchi, K. *Bioorg. Med. Chem. Lett.* **2003**, *13*.
- Asaki, T.; Hamamoto, T.; Sugiyama, Y.; Kuwano, K.; Kuwabara, K. *Bioorg. Med. Chem.* **2007**, doi:doi:10.1016/j.bmc.2007.08.010.
- Pietraszkiewicz, M.; Jurczak, J. *Tetrahedron* **1984**, *40*, 2967.
- Burns, S. A.; Corriu, R. J. P.; Huynh, V.; Moreau, J. J. E. *J. Organomet. Chem.* **1987**, *333*, 281.
- Yamamoto, K.; Yamazaki, S.; Murata, I. *J. Org. Chem.* **1987**, *52*, 5239.
- Sasaki, T.; Kanematsu, K.; Murata, M. *J. Org. Chem.* **1971**, *36*, 446.
- Laakso, P. V.; Robinson, R.; Vandrewala, H. P. *Tetrahedron* **1957**, *1*, 103.
- Tohda, Y.; Eiraku, M.; Nakagawa, T.; Usami, Y.; Ariga, M.; Kawashima, T.; Tani, K.; Watanabe, H.; Mori, Y. *Bull. Chem. Soc. Jpn.* **1990**, *63*, 2820.
- Crochet, R. A.; Dewitt, B. C. *Synthesis* **1974**, 55.
- SanMartín, R.; Marigorta, E. M.; Dominguez, E. *Tetrahedron* **1994**, *50*, 2255.
- Stitham, J.; Stojanovic, A.; Merenick, B. L.; O'Hara, K. A.; Hwa, J. *J. Biol. Chem.* **2003**, *278*, 4250.
- Halgren, T. A. *J. Comput. Chem.* **1996**, *17*, 490.
- Muchmore, S. W.; Souers, A. J.; Akritopoulou-Zanze, I. *Chem. Biol. Drug Des.* **2006**, *67*, 174.